



Cite this: *Environ. Sci.: Adv.*, 2024, **3**,  
470

## Weathering of agricultural polyethylene films in cold climate regions: which parameters influence fragmentation?†

Laura Rowenczyk, \* Heidi Jahandideh, Nicholas Lin and Nathalie Tufenkji

Plastic agricultural mulch films are used to improve the productivity of cultivable fields; however, their weathering and fragmentation could lead to release of microplastics and nanoplastics, both of which are considered potential health and environmental hazards. In this study, we examined the changes in physical and chemical properties of various plastic mulch films as they underwent different weathering processes. For this purpose, three commercially available polyethylene mulch films (one clear and two dark films) were evaluated under the following weathering conditions: laboratory treatments to evaluate the impacts of moisture, ultraviolet irradiation, pH, and freeze–thaw, as well as natural weathering conditions of a cold climate region. The morphologies and physicochemical properties of the polyethylene films were systematically studied following exposure to controlled and natural weathering. The three films, one of which was marketed as UV-resistant, underwent significant modifications. All weathered films were found to have increased surface roughness, suggesting that this could be the origin of microplastics or nanoplastics. While the dark pigments in the UV-resistant film protected the film against UV oxidation to some degree, they did not prevent deterioration caused by other types of weathering such as moisture, freeze–thaw, or natural weathering. The results of this study provide insights to understanding the fragmentation of polyethylene films into microplastics in winter and cold climate conditions.

Received 31st August 2023  
Accepted 29th January 2024

DOI: 10.1039/d3va00255a  
[rsc.li/esadvances](http://rsc.li/esadvances)

### Environmental significance

The widespread use of plastic items has been identified as a subject of great concern in modern society. In the case of plastic mulches found on arable fields, it is legitimate to wonder about the fate and weathering of such plastic films. Indeed, once in the environment, the physico-chemical properties of plastic films could rapidly change over time, leading to phenomena such as their fragmentation into microplastics or the leaching of plastic additives. This study aims to assess the conditions leading to the acceleration of such phenomena in order to mitigate uptake into crops and potential human health impacts.

## 1 Introduction

To support a growing global population, agricultural output must significantly improve in the coming years. One of the approaches taken by the agricultural industry to tackle this challenge is utilizing agricultural mulch films. These films are used as means to maintain soil moisture, suppress weeds, reduce nutrient loss and regulate soil temperature,<sup>1,2</sup> and ultimately, to increase the productivity of cultivable fields. Notably, mulch films can be applied in cold climate regions during parts of the winter season to avoid crop degradation due to frost.<sup>3</sup> From 2015 to 2020, the market size for mulch films grew exponentially with a compound annual growth rate of 6.5%.<sup>4</sup>

Today, mulch films are predominantly manufactured as polypropylene or polyethylene films.

The use of large quantities of plastic materials comes with some concerns. For example, release of polyolefins into cultivable soils could degrade soil quality over time.<sup>5</sup> In a study by Qi *et al.*, it has been shown that the presence of low density polyethylene (LDPE) films affects soil properties such as porosity, pH, water repellency, and even field capacity.<sup>6</sup> The authors proposed that LDPE films could fragment into microplastics and nanoplastics which migrate into soil, thereby modifying soil properties. While plastic fragmentation when exposed to environmental stressors is well known, the fate of the polyolefin films themselves is poorly described in the literature.<sup>7,8</sup> Nevertheless, it has been estimated that the microplastic loadings in US farmland could be as high as 9 to 63 tonnes per hectare.<sup>9</sup> Moreover, experiments conducted by Scheurer and Bigalke found up to 55.5 mg kg<sup>-1</sup> of plastic particles (125–500 µm) in soils in Switzerland<sup>10</sup> whereas Zhang *et al.* found a maximum of

Department of Chemical Engineering, McGill University, 3610 University Street, Montréal, Québec, H3A 0C5, Canada. E-mail: [laura.rowenczyk@polymtl.ca](mailto:laura.rowenczyk@polymtl.ca)

† Electronic supplementary information (ESI) available. See DOI: <https://doi.org/10.1039/d3va00255a>



0.54 mg kg<sup>-1</sup> of polyethylene particles (>100 µm) in soils tested in China.<sup>11</sup> It is worth noting that there are no reports on the occurrence of smaller plastic particles (*i.e.*, nanoplastics) which could be responsible for a considerable portion of soil pollution and a substantial hazard in the agricultural soils. Owing to their small size, nanoplastics can be ingested by soil fauna such as earthworms and insects,<sup>12</sup> or taken up by plants,<sup>13</sup> while acting as vectors for pollutants.<sup>14,15</sup> It is thus essential to obtain experimental data with respect to the fragmentation of plastic mulch in contact with soils, though the isolation, identification and quantification of nanoplastics is not trivial.<sup>16,17</sup>

One of the strategies to study the generation of micro- and nanoplastics from plastic items is to follow the fragmentation of these items during their weathering. In the last decades, plastic fate and degradation have been carefully monitored and studied in aqueous natural environments. In the ocean, plastics are heavily degraded from the combined action of erosion by ocean waves and irradiation by sunlight.<sup>18</sup> At the microscopic scale, material crystallinity and oxidation significantly increase.<sup>19</sup> At the molecular scale, the arrangement of the polymer molecules is also modified.<sup>20</sup> Evidently, natural weathering conditions combine complex effects of multiple processes that impact various physicochemical parameters of the plastics at different timescales.

While plastic weathering and fragmentation induced by UV irradiation is well described in the literature,<sup>21</sup> the effects of low temperatures (representative of winter seasons and cold climate regions) or low pH (representative of acidic precipitation) are not well understood.<sup>22</sup> It can be hypothesized that these phenomena could also affect the physicochemical and structural properties of agricultural mulch. To address this, the present study aims to evaluate weathering under natural and artificial treatments of three commercially available polyethylene agricultural films formulated with different additives. In the laboratory, weathering conditions were controlled to evaluate the individual impacts of moisture, UV irradiation, pH, and freeze-thaw on the physicochemical properties of the films. These artificial treatments were then compared to naturally weathered plastic mulch films exposed outdoors during the winter season in Montreal, Canada. The macro- and micro-structures and physicochemical properties of the films were monitored and compared at different scales. This study provides new data to evaluate and understand the weathering and fragmentation of agricultural plastic films.

## 2 Materials and methods

### 2.1 Materials

Anhydrous ethanol (EtOH) was purchased from Commercial Alcohols (Ontario, Canada) and diluted in reversed osmosis (RO) water to 70% v/v. The phosphate buffer (pH 4) consisted of 800 mL K<sub>2</sub>HPO<sub>4</sub> solution in ultrapure water (0.2 M) mixed with 200 mL of citric acid (0.1 M) to reach the final pH of 4.08 ± 0.05. Three commercial polyethylene films used as plastic mulch for agricultural purposes were purchased from two different manufacturers: film 1 (F1) is a dark film (P1025/3B, Frost King, Thermwell Products Co., NJ, USA – thickness 0.07 mm), film 2

(F2) is a translucent film (P1020/3, Frost King, Thermwell Products Co., NJ, USA – thickness 0.07 mm) and film 3 (F3) is a dark film marketed as UV-resistant (NH-3100, Warp Brothers, Inc., IL, USA – thickness 0.04 mm).

### 2.2 Weathering procedures

For laboratory weathering, the three films were cut into 2 cm × 2 cm squares. Next, the squares were rinsed with RO water then weathered for 20 weeks following one of the conditions summarized in Table 1. In the case of UV irradiation (UVRO and UV4), monochromatic bulbs were used (~35 W m<sup>-2</sup>), which meant that no direct comparison could be made with solar irradiation (see Calculation S1†).

Naturally weathered films were cut into similar sized squares post treatment. For brevity, samples are referenced throughout the manuscript by abbreviations based on the type of film (F1, F2, or F3) followed by their type of weathering treatment (dC, wC, UVRO, UV4, FT, or Nat). Prior to analyzing the films, they were quickly cleaned by rinsing with 70% EtOH.

### 2.3 Characterization of films

**2.3.1 Scanning electron microscopy (SEM).** Morphology of the plastic films was monitored by SEM. For this purpose, plastic film squares were cut in quarters and placed on carbon tape then sputter-coated with a 4 nm layer of platinum (EM ACE600, Leica Microsystems). Samples were then imaged using a field emission environmental SEM (high vacuum, 10 kV beam, FEI Quanta 450). Both the sputter coater and microscope are located at the Facility for Electron Microscopy Research (FEMR) at McGill University.

**2.3.2 Fourier-transform infrared spectroscopy (FTIR).** A Spectrum II Fourier Transformed Infrared (FTIR) spectrometer in attenuated total reflection (ATR) mode was employed (PerkinElmer, MA, USA) to scan the surface chemical bonds of the films pre and post treatments. Spectra were acquired in the 4000–500 cm<sup>-1</sup> region using 16 scans and a spectral resolution of 4 cm<sup>-1</sup>. For each condition, three squares were randomly selected and both sides were analyzed once by FTIR (total of 6 measurements per condition). The ATR correction was processed by the instrument software (Spectrum 10 STM, PerkinElmer). All spectra were normalized using Orange data mining software (version 3.24.0). The carbonyl index (CI) was defined as the area of the carbonyl band (1780–1700 cm<sup>-1</sup>) divided by the area of the methylene band (1550–1230 cm<sup>-1</sup>).<sup>19</sup> The unsaturated bond index (UBI) was defined as the area of the carbon double bonds (1680–1600 cm<sup>-1</sup>) divided by the area of the methylene band (1550–1230 cm<sup>-1</sup>).<sup>23</sup>

**2.3.3 Thermogravimetric analysis (TGA).** The additive/polymer ratio was evaluated for each film using a thermogravimetric analyzer (TGA Q500, TA Instruments, DE, USA). Approximately, 2–5 mg of each sample was placed in a platinum pan (100 µL). A temperature ramp analysis proceeded up to 600 °C at 20 °C min<sup>-1</sup> under N<sub>2</sub> as carrier gas. At 600 °C, the carrier gas was switched to air and a temperature ramp was then proceeded up to 800 °C at 20 °C min<sup>-1</sup> to pyrolyze the residue. The mass loss curves were normalized and integrated on



Table 1 Summary of weathering treatments performed in this study

| Type of weathering                                 | Sample abbreviation       | Procedure   |
|--|---------------------------|---|
| Dry control (dC)                                   | F1dC, F2dC and F3dC       | Plastic squares were stored in a hermetically sealed glass dish (dimension: 20 × 10 cm) at room temperature in the dark   |
| Wet control (wC)                                   | F1wC, F2wC and F3wC       | Plastic squares were floating in 250 mL of RO water in a hermetically sealed glass dish (dimension: 20 × 10 cm, water level: 1.5 cm) and stored at room temperature in the dark   |
| UV-weathered films in reverse osmosis water (UVRO) | F1UVRO, F2UVRO and F3UVRO | Plastic squares were floating in 250 mL of RO water in a hermetically sealed glass dish (dimension: 20 × 10 cm, water level: 1.5 cm) and irradiated in a UV chamber (306 nm; Topbulb G15T8E, 350 nm; Topbulb, Eiko F15T8/BL and 365 nm; Hikari Lamps) with orbital agitation (35 rpm) at 25 °C              |
| UV-weathered films at pH 4 (UV4)                   | F1UV4, F2UV4 and F3UV4    | Plastic squares were floating in 250 mL of pH 4 phosphate buffer in a hermetically sealed glass dish (dimension: 20 × 10 cm, water level: 1.5 cm) and irradiated in a UV chamber (306 nm; Topbulb G15T8E, 350 nm; Topbulb, Eiko F15T8/BL and 365 nm; Hikari Lamps) with orbital agitation (35 rpm) at 25 °C |
| Freeze-thawed films (FT)                           | F1FT, F2FT and F3FT       | Plastic squares were stored in a hermetically sealed glass dish (dimension: 20 × 10 cm) frozen at -11 °C for 20 weeks. When back at ambient temperature, 250 mL of RO water was added into the dish. Here, for the sake of brevity, we refer to this condition as "freeze-thaw"                             |
| Naturally weathered films (Nat)                    | F1Nat, F2Nat and F3Nat    | Plastic films (~30 cm × 30 cm) were placed outdoors on natural soil in the Montreal area from November 14, 2020 to April 2, 2021 for 20 weeks (Fig. S1)   |

Universal Analysis (Advantage Software, v5.5.24, TA Instruments) following the recommendations of PerkinElmer for the characterization of polyolefins to obtain the volatile compounds (between 0 and 350 °C), polymer (between 350 and 550 °C) and residual carbons (between 550 and 800 °C).<sup>24</sup> Since the remaining mass at 800 °C varied around 0% of initial mass (±5%) and seemed to be more likely related to a measurement artefact, the TGA curves were normalized prior to data analysis to enable the comparison between samples. This experiment was repeated three times.

**2.3.4 Differential scanning calorimetry (DSC).** Polymer properties were evaluated using a differential scanning calorimeter (DSC Q2000, TA Instruments, DE, USA). About 1 mg of the sampled film was placed in an aluminum hermetic pan. The procedure to characterize the phase transition of a polymer was adapted from a previously published work.<sup>19</sup> Briefly, the temperature of the sample was stabilized at -50 °C for 5 min and then, increased to 200 °C at 10 °C min<sup>-1</sup>. Then, the temperature was stabilized at 200 °C for 5 min and then decreased to -50 °C at 10 °C min<sup>-1</sup>. This cycle was repeated twice. The first cycle provides the crystallinity history of the polymer and depicts the weathering of the film. With the objective of characterizing the crystallinity of the films, the melting peaks of the first cycles were integrated between 25 and

142.5 °C using Universal Analysis (Advantage Software, v5.5.24, TA Instruments) to obtain the melting enthalpy.

The crystalline fraction was calculated as the ratio between melting enthalpy of the samples and the melting enthalpy of a theoretical 100% crystallized polyethylene, *i.e.*, 290 J g<sup>-1</sup>.<sup>25</sup> Values were corrected by the percentage of polymer in the films obtained by TGA (Table ESI 4†). The experiment was repeated three times.

**2.3.5 Contact angle goniometry.** Contact angles were measured by the sessile-drop method using an OCA 15EC goniometer and accompanying software SCA 15 (DataPhysics Instruments GmbH, Germany). The angle formed by a 5 µL droplet of ultrapure water (polar component: 50.7 mN m<sup>-1</sup>; dispersive component: 22.1 mN m<sup>-1</sup>) was captured by the Young–Laplace fitting within 10 s after droplet deposition. Three measurements were performed for each side of at least three samples (for a total of at least 18 measurements per condition).

## 2.4 Statistical analysis

Unless otherwise stated, the statistical software package JASP v0.16.4 was employed for all statistical analysis. *P* < 0.05 denote a statistically significant result. Figure captions provide the statistical treatment for each type of experiment.



### 3 Results

#### 3.1 Macroscopic variations in physical appearance

For all weathering processes tested, the films underwent no visible changes on a macroscopic scale. With the exception of several plastic squares that were fused together during the UV4 treatment – and thereafter excluded from the study – no surface crack, porosity, and/or colour variation were observable with unaided visual inspection (Fig. S2†). There were also minimal differences in mass of the plastic squares before and after weathering (Fig. S3†).

#### 3.2 Changes in microscopic morphology of the films

Confocal laser scanning profilometry did not show any significant variation in mean area surface roughness between weathered and unweathered films (Fig. S4†). SEM at higher spatial resolution allowed visualization of surface features. As can be seen in Fig. 1, the surfaces of dry control films were smooth for all three films. However, after 20 weeks in water (wet control), microscopic fragmentation in the form of flakes was observed on the films' surfaces. These fragments measured up to 10 µm for F3. For the UVRO, UV4, FT, and Nat treatments, morphology and roughness of the films were even more drastically altered. Interestingly, qualitative observations across all films suggest that UV irradiation in RO water and natural weathering conditions were the most impactful treatments, while weathering at cold temperatures (freeze–thaw) seemed to generate relatively little fragmentation.

#### 3.3 Evolution of the chemical composition of the films' surfaces

The chemical composition of the film surfaces was characterized by ATR-FTIR (Fig. 2, S5 and S6†). Several bands characteristic of polyethylene can be identified. Two intense bands at

2915 cm<sup>−1</sup> and 2846 cm<sup>−1</sup> correspond to the asymmetric and symmetric stretching of the methylene groups, respectively and the next band at 1460 cm<sup>−1</sup> corresponds to the bending and rocking of the CH<sub>2</sub> groups<sup>26</sup> (Fig. S5†). Finally, between 730 and 718 cm<sup>−1</sup>, there is a doublet corresponding to the bending of the CH<sub>2</sub> groups for alkenes and markers of the polymer crystallinity.<sup>27</sup> In addition to these common bands, an unusual intense band is found at 875 cm<sup>−1</sup> for the films (Fig. S5†) that matches well with the bending of the RR'C=CH<sub>2</sub> unsaturation in alkenes.<sup>28</sup> Moreover, a shoulder is also visible at 1368 cm<sup>−1</sup> which could be the marker of the bending of the C–H doublet in the –C–(CH<sub>3</sub>)<sub>3</sub> moiety.<sup>29</sup> These two last bands could either represent markers of early-stage weathering due to the formulation of the material or simply from the presence of additives in the plastic matrices.<sup>19</sup>

After each weathering treatment, new bands were observable in the regions from 1800 to 1550 cm<sup>−1</sup> (Fig. 2) and from 1200 to 900 cm<sup>−1</sup> (Fig. S6†). As described in the literature, the early stage of polyethylene oxidation usually leads to the oxidation of ketones (at 1720 cm<sup>−1</sup>)<sup>19</sup> which was slightly visible for F1 and F2 after neutral and acidic UV irradiation and after natural weathering. The second oxidation step usually relates to the formation of carboxylic acids and esters,<sup>30</sup> that can be observed by its characteristic band assigned to C=O stretching vibrations of the carbonyl (1718–1713 cm<sup>−1</sup>). This band is visible for F2 after neutral and acidic UV irradiation. Additionally, the characteristic bands of the C–O stretches (1080 and 1018 cm<sup>−1</sup>)<sup>31</sup> were mainly visible in F1UV4, F1Nat, F2UV4, F2Nat, and F3Nat, indicative of the advanced oxidation stage of these samples (Fig. S6†). Finally, the last stage of degradation is marked by the presence of bands assigned to C=O stretching vibrations in lactones (1780 cm<sup>−1</sup>)<sup>32</sup> which were only found in F1 and F2. Since these two bands were already slightly observed for the control films, it cannot be concluded that these chemical moieties were formed during the weathering of the films; they

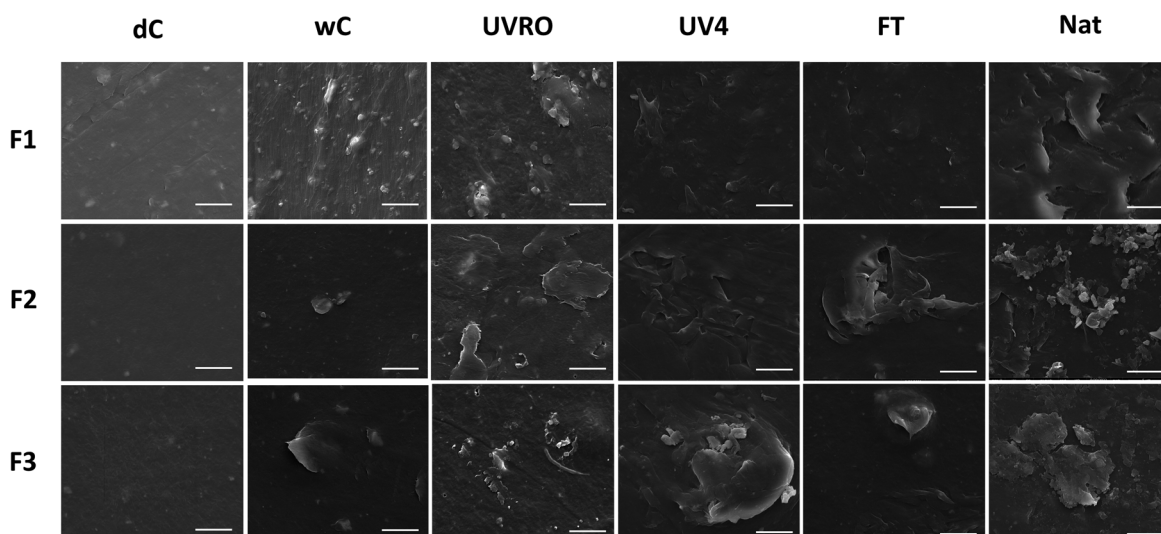


Fig. 1 SEM micrographs (5000 $\times$  magnification) of the surface of the three plastic films weathered under different conditions for 20 weeks. Scale bars for all images represent 5 µm.



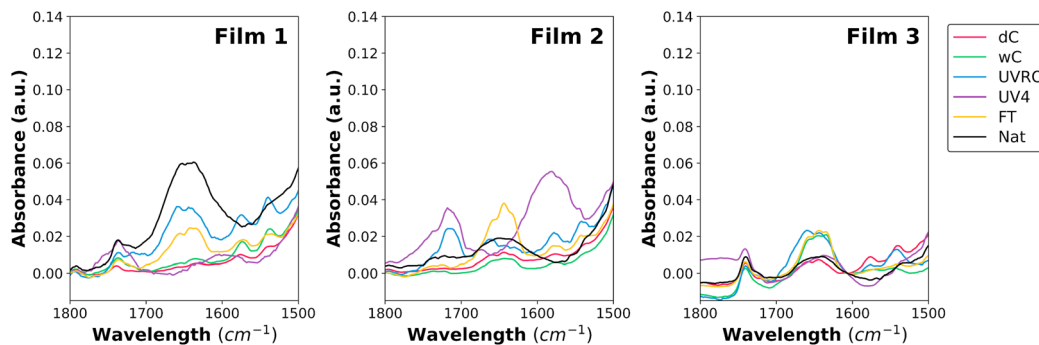


Fig. 2  $1800\text{--}1500\text{ cm}^{-1}$  regions of the FTIR spectra obtained for the three films after the different weathering treatments. Each spectrum is an average signal obtained from 6 spectra resulting from the analysis of points on different plastic squares.

could be attributed to the presence of additives in the plastic matrices.

Besides the appearance of specific oxidation moieties, the large bands between  $1660$  and  $1632\text{ cm}^{-1}$  that are made of convoluted peaks and visible for F1UVRO, F1FT, F1Nat, F2FT, F2Nat, F3wC, F3UVRO, and F3FT could be the result of the formation of  $\text{C}=\text{C}$  during chain scission.<sup>33</sup> Moreover, in the case of F2, a strong band ( $1600\text{--}1550\text{ cm}^{-1}$ ) appeared after acidic UV-weathering and could be the marker of nitroxides resulting from the oxidation of hindered amine light stabilizers (HALS) which are common additives used to stabilize polyethylene films.<sup>34</sup>

The carbonyl index (CI), a parameter commonly used to quantify the weathering extent of plastic polymers in the literature,<sup>35</sup> was calculated for each film and weathering condition using the FTIR measurements. In general, the results indicated that weathering treatments with water and freeze-thaw led to insignificant increase of the CI value of the three films (Fig. 3A). CI values were significantly higher for F1UV4, F2UVRO and F2UV4 compared to their respective dry controls. This result highlights that the UV treatment was likely responsible for the surface oxidation of the films by generating carbonyl groups. F3, which was marketed as a UV-resistant film, indeed seemed to resist oxidation more effectively than the other two films under

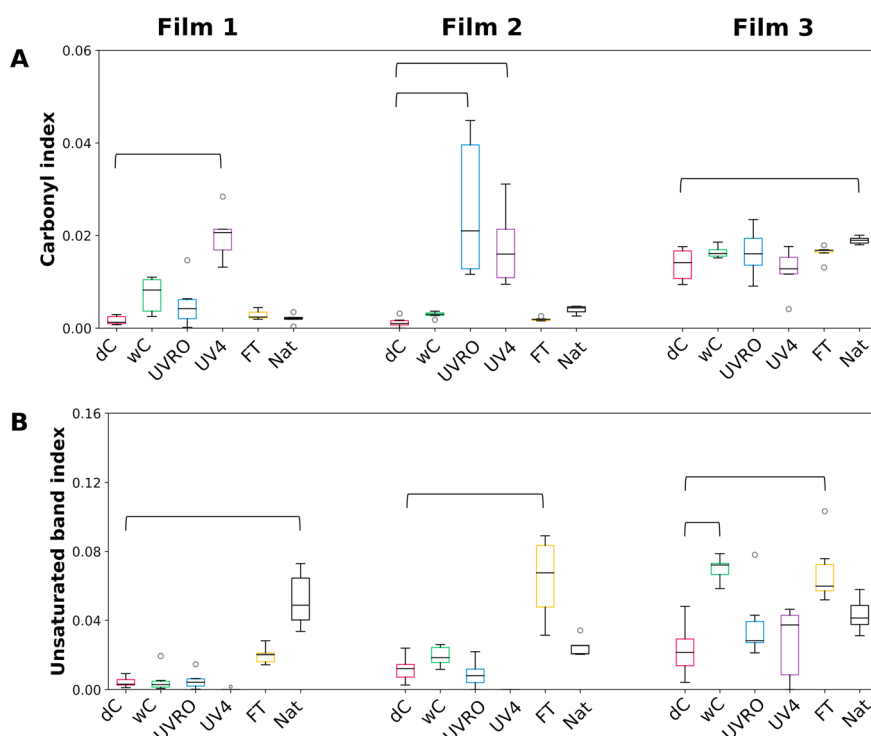


Fig. 3 Carbonyl (A) and unsaturated band (B) indexes of the films after diverse weathering treatments. Medians are represented by the horizontal black lines.  $\circ$  = outliers. The thicker horizontal brackets link the values significantly different from the value of the corresponding dry control (dC) according to a *post hoc* comparison (Kruskal–Wallis, Dunn's *post hoc* comparisons, Bonferroni correction,  $p < 0.05$ ,  $n = 6$ ). Full statistical comparisons are provided in Tables S1 and S2.<sup>†</sup>



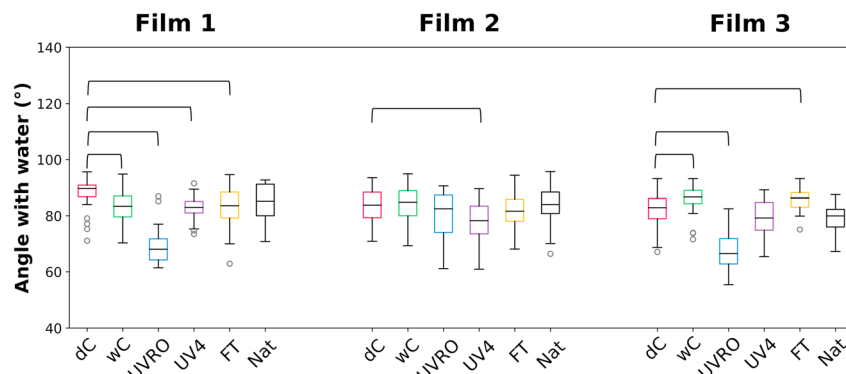


Fig. 4 Contact angle formed by the deposition of a drop of water on the three films after different weathering treatments. Medians are represented by the black horizontal lines.  $\circ$  = outliers. The thick horizontal brackets link the values significantly different from the value of the corresponding dry control (dC) according to a *post hoc* comparison (Kruskal–Wallis, Dunn's *post hoc* comparisons, Bonferroni correction,  $p < 0.05$ ,  $n \geq 27$ ). Full statistical comparison is provided in Table S3.†

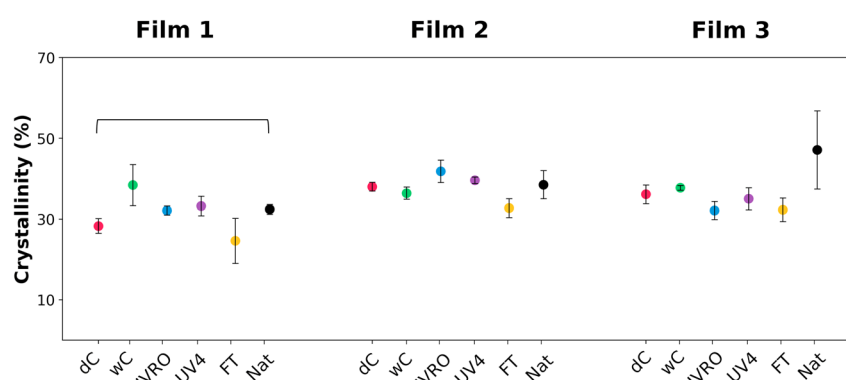


Fig. 5 Crystallinity of the films with different weathering treatments. The horizontal brackets link the values significantly different from the value of the corresponding dry control (dC) according to a *post hoc* comparison ( $t$ -test,  $p < 0.05$ ,  $n = 3$ ).

UV exposure. However, its CI increased slightly with natural weathering compared to its dry control suggesting that the combination of other factors including drastic temperature changes, presence of biotic and abiotic stressors in the environment and the deposition of rain and snow over time played a role in its CI increase.

Importantly, the CI method does not take into account the formation of  $\text{C}=\text{C}$  on the surface of the polymer ( $1660\text{--}1632\text{ cm}^{-1}$ ) which could also be a marker of the material weathering.<sup>36</sup> For this purpose, the unsaturated band index (UBI) can be employed as it provides a relative quantification of these types of carbon unsaturations in polymers.<sup>23</sup> As seen in Fig. 3B, the level of unsaturation is higher in F1Nat, F2FT, F3wC, and F3FT compared to their respective dry control films. Since FT is generally considered to be a physical and not a chemical alteration, researchers have found that the freeze-thaw process can cause polymer physical alterations leading to the release of plasticizers.<sup>37</sup> In this study, it is suspected that the release of certain additives towards the mulch surface could lead to the appearance of unsaturation.

While NaT, FT and wC treatments generally produced low CI values, when combined with the UBI information, it becomes apparent that every treatment led to noticeable chemical modifications on at least one of the three film types.

### 3.4 Evolution of film wettability

Changes in both the microscopic fragmentation and chemical compositions described earlier can potentially lead to changes in film surface wettability. To this end, the water contact angles of the films were measured before and after weathering treatments (Fig. 4). The water contact angles for the three dry control films (F1dC:  $87.9 \pm 5.3^\circ$ ; F2dC:  $83.6 \pm 6.1^\circ$ ; F3dC:  $82.1 \pm 6.6^\circ$ ) were consistent with values reported for polyethylene films at room temperature ( $88 \pm 2^\circ$ ).<sup>38</sup> The slight deviation observed between the films tested and literature value could be due to the additives used in agricultural films. As expected, the various weathering treatments impacted the wettability of the plastic films studied here. wC, UVRO, UV4, and FT treatments each significantly changed the wettability of two out of the three films. Surprisingly, natural weathering did not have a significant impact on film wettability on any of the three films tested here.

### 3.5 Changes in polymer crystallinity

Thermogravimetric analysis (TGA) of control films was performed to elucidate their polymeric compositions (Fig. S7†). The single smooth decline in derived weight with a maximum rate at 470–485 °C was consistent with the simultaneous polyethylene chain scission and branching through free-radical mechanisms described in the literature.<sup>39,40</sup> The percentages of polymer calculated using the weight loss curves was found to be similar for the three films suggesting that they contain comparable polymer to additives ratio (Table S4†).

The melting curves obtained by DSC showed characteristic endotherms of polyethylene melting (Fig. S8†).<sup>19</sup> For the control films, the starting melting point is observed to be as low as 50 °C (shoulder 1). The second and third shoulders are observed at ~105 °C and 115 °C, respectively. And finally, the fourth and main melting episode is reached between 119 °C and 123 °C for each film. No major variation in terms of melting temperature was observed among the samples, except that the starting melting temperature is usually found to be higher for weathered samples (Table S5†). The melting curves of the weathered films showed similar endothermic peaks regardless of the weathering treatments. However, it could be noted that the third peak (113–118 °C) was relatively more intense for the samples after UV-weathering compared to the control films. Only a slight increase in terms of crystallinity was observed between F1dC and F1Nat (Fig. 5).

## 4 Discussion

In this study, we subjected three polyethylene-based commercial agricultural mulch films to various weathering treatments. Although discoloration and increase of the surface porosity have been previously reported after long-term natural weathering of plastic litter in a marine environment,<sup>19</sup> herein, we report no macroscopic variation for the films regardless of the weathering treatments. One major difference between these studies is their time scales. The films studied here were only weathered for 20 weeks while the degraded plastic litter found in the ocean had been subjected to weathering conditions for several decades.<sup>41</sup>

The surfaces of all three plastic films were impacted on a microscopic scale upon weathering. The surface of each weathered film showed fragmentation in the form of microscopic flakes. These particulates are likely the origin of microplastics generated from these plastic films. This observation is consistent with previous reports on weathered plastic items retrieved from the ocean<sup>19</sup> and under laboratory conditions.<sup>42</sup> Although this study cannot provide quantitative data regarding the formation of microplastics by such plastic films, it presents the insight that even short-term weathering treatments promote the fragmentation of particulates on the surfaces of the films. In other words, this observation shows that freshwater exposure for only 20 weeks is sufficient to generate particles from polyethylene films. This corroborates a proposal by Julianne *et al.* suggesting that water promotes the fragmentation of low density polyethylene by acting as a plasticizer and reducing the

plastic surface rigidity.<sup>43</sup> Consequently, the ability of the weathered polymer to resist crack initiation and propagation is considerably lowered in the presence of water.

Generally, surface cracks are more likely to occur when the mechanical strength in the surface layer cannot withstand the anisotropic internal stress.<sup>44</sup> Additionally, surface physico-chemical changes, such as oxidation, chain scission or crystallinity variation could also lead to the formation of fine cracks. However, the relations between these parameters and plastic fragmentation remain unclear. Some researchers have highlighted that surface cracks appear when the crystallinity of high-density polyethylene decreases<sup>42</sup> while others have suggested that the crystallization of polyolefins generates local volume reductions and consequently, crack formation.<sup>45</sup> Since fragmentation was observed for all samples regardless of their weathering conditions, the role of crystallinity variations in the polymer fragmentation cannot be concluded.

The oxidation of weathered films was also characterized and mainly observed on weathered F1 and F2 after the UV weathering treatments through the formation of carbonyl groups. This is in accordance with the formation of main oxidation products after radical photo-oxidation of polyolefins in the presence of O<sub>2</sub> and initiated by metal impurities.<sup>36</sup> The F1 and F2 films studied here were similar in chemical composition and differed in color; however, based on our findings, the dark pigments in F1 did not provide a significant barrier against UV irradiation. In contrast, F3 which was marketed as a UV-resistant film, did not show the same kind of chemical deterioration after UV exposure. Therefore, it can be safely assumed that the addition of light stabilizers<sup>34</sup> can minimize penetration of UV irradiation through the material. In the case of the freeze-thawed and naturally weathered treatments, no measurable amounts of C=O groups were formed but quantitative amounts of C=C groups were detected in all three films. These particular C=C bonds are also connected to the polyolefin oxidation during environmental and artificial weathering.<sup>46</sup> It was suggested that there is a dominance of two different reactions during weathering leading to the formation of carbonyl groups or the formation of aldehydes and polymer fragments with terminal vinyl groups, respectively.<sup>47</sup> This shows the importance of including UBI as an indicator of plastic degradation (*i.e.*, formation of vinyl groups) in addition to CI. The sole reliance on the CI may mislead the analysis of plastic degradation under natural conditions.

It is well known that surface oxidation affects surface properties such as wettability. While no significant change in contact angle is reported for most films upon weathering, most of the weathered films that presented any change in their wettability, became more hydrophilic. This increase in surface polarity was detected in many of the UV treatments, in agreement with their level of oxidation. It is worth mentioning that surface polarity, CI and UBI are weathering markers that should be interpreted with caution. Firstly, CI and UBI values computed using ATR-FTIR are surface characterization methods. In the context of plastic weathering, the surfaces were eroded, as shown by SEM observation, exposing the pristine and/or non-oxidized layers.<sup>48</sup> In the case of contact angle analysis, the porosity of the



weathered surfaces could decrease the repeatability of the measurements and impact the quality of the results.

Bulk measurements and analyses, such as DSC and TGA, were also used during this study and provide a more global assessment of the polymer state. To understand the results provided by these techniques, it is essential to consider the polymers within the films as a mixture of long molecules with various molecular weights and branching structures.<sup>36</sup> Consequently, analyses of polymers by DSC provide a melting range rather than a melting point. Here, it was found that the starting melting temperature of the films was higher for weathered samples. Chabira *et al.* also observed an increase of the melting temperature after weathering of polyethylene films.<sup>49</sup> This phenomenon could indicate: (i) the areas made of shorter polymer chains were reorganized during weathering, and/or (ii) the linearity of the polymer has increased due to the sectioning of polymer branches. However, in this study, no significant modification of the crystallinity was observed after weathering.

Weathering studies are often performed on pristine polymers that do not contain any additives. However, these ingredients can play an important role during the aging of the plastic items. Here, the specific three agricultural mulches were chosen to compare the effect of dark pigments (F1 *versus* F2) and UV stabilizers (F2 *versus* F3) on plastic degradation. The outcome of these investigations can be summarized as follows. Firstly, the dark film (F1) showed a lower CI value but a greater change in wettability compared to the transparent film (F2). Secondly, as expected, the UV-resistant film (F3) was noticeably more resistant to UV-irradiation compared to the other two films. However, while the additives protected the films against UV oxidation to some degree, they did not prevent deterioration caused by other types of weathering such as moisture, freeze-thaw, or natural weathering. Finally, it should be assumed that multiple individual weathering phenomena take place during plastic weathering in the natural environment. Other types of natural interactions, such as microbial, could also influence the polymer decomposition in the natural environment, as it could be the case during the natural weathering of this study.<sup>50,51</sup> Thus, while this study provides some insights on the individual effects of selected environmental factors under controlled laboratory conditions, it does not perfectly mimic conditions that mulch films experience when they are used in agricultural crop production.

## 5 Conclusions

In this study, we weathered three commercially available agricultural polyethylene mulch films. Two of the films were of the same brand and differed primarily in color while a third was marketed as UV-resistant. We compared the extent of physico-chemical changes of the films as a result of laboratory weathering and natural weathering representative of a cold climate region. Laboratory exposures to moisture, UV-irradiation, and freeze-thaw as well as natural weathering all resulted in quantifiable modifications to the physicochemical properties of the films' surfaces. Based on our electron microscopy observations, all weathered films were found to have particulates on their

surfaces, suggesting that this could be the origin of microplastics or nanoplastics fragmentation. Based on our physico-chemical characterizations, it was unclear whether addition of pigmentation of a dark plastic film had appreciable functional benefits, and while the additives in the UV-resistant film indeed protected the film against UV oxidation to some degree, they did not prevent deterioration caused by other types of weathering such as moisture, freeze-thaw, or natural weathering.

## Author contributions

Laura Rowenczyk: conceptualization, methodology, investigation, validation, formal analysis, visualization, writing – original draft, writing – review & editing. Heidi Jahandideh: conceptualization, methodology, investigation, validation, formal analysis, writing – review & editing. Nicholas Lin: conceptualization, methodology, investigation, validation, analysis, writing – review & editing. Nathalie Tufenkji: conceptualization, funding acquisition, writing – review & editing, supervision.

## Conflicts of interest

The authors declare no competing conflicts of interest.

## Acknowledgements

N. T. acknowledges the support of the Canada Research Chairs program, the Canada Foundation for Innovation, the Killam Research Fellowship program, the Natural Sciences and Engineering Research Council of Canada (NSERC) and the Fonds de recherche du Québec – Nature et technologies (grant no. 286120 and 328469). L. R.'s postdoctoral fellowship is supported by Merinov, Mitacs Canada and Réseau Québec Maritime. H. J. and N. L. each hold an NSERC CGS-Doctoral Scholarships and EUL scholarships, and McGill Engineering Doctoral Awards. H. J. is additionally supported by the Vadasz Doctoral Fellowship and an NSERC CREATE PURE Award. The authors would like to acknowledge the assistance of Caroline Kouri during data collection.

## Notes and references

- 1 E. K. Liu, W. Q. He and C. R. Yan, 'White revolution' to 'white pollution'—agricultural plastic film mulch in China, *Environ. Res. Lett.*, 2014, **9**, 091001.
- 2 T. Hofmann, S. Ghoshal, N. Tufenkji, J. F. Adamowski, S. Bayen, Q. Chen, P. Demokritou, M. Flury, T. Hüffer, N. P. Ivleva, R. Ji, R. L. Leask, M. Maric, D. M. Mitrano, M. Sander, S. Pahl, M. C. Rillig, T. R. Walker, J. C. White and K. J. Wilkinson, Plastics can be used more sustainably in agriculture, *Commun. Earth Environ.*, 2023, **4**(1), 332.
- 3 S. A. Rao, P. Singh and T. Gonsalves, Black plastic mulch affects soil temperature and yield of sweet potato under short season temperate climates, *Int. J. Veg. Sci.*, 2022, **1**–12, DOI: [10.1080/19315260.2022.2111625](https://doi.org/10.1080/19315260.2022.2111625).
- 4 Mulch Films Market by Type (Clear/Transparent, Black, Colored, and Degradable), by Application (Agricultural Farms,

and Horticulture), by Element, LDPE, *Global Trends and Forecast to, 2020, 2023*, [https://www.marketsandmarkets.com/Market-Reports/mulch-films-market-220908278.html?utm\\_source=PRnewswires&utm\\_medium=Referral&utm\\_campaign=PRnewswire](https://www.marketsandmarkets.com/Market-Reports/mulch-films-market-220908278.html?utm_source=PRnewswires&utm_medium=Referral&utm_campaign=PRnewswire), (accessed January 2024).

5 Z. Steinmetz, C. Wollmann, M. Schaefer, C. Buchmann, J. David, J. Tröger, K. Muñoz, O. Frör and G. E. Schaumann, Plastic mulching in agriculture. Trading short-term agronomic benefits for long-term soil degradation?, *Sci. Total Environ.*, 2016, **550**, 690–705.

6 Y. Qi, N. Beriot, G. Gort, E. H. Lwanga, H. Gooren, X. Yang and V. Geissen, Impact of plastic mulch film debris on soil physicochemical and hydrological properties, *Environ. Pollut.*, 2020, **266**, 115097.

7 N. Kalogerakis, K. Karkanorachaki, G. C. Kalogerakis, E. I. Triantafyllidi, A. D. Gotsis, P. Partsinevelos and F. Fava, Microplastics Generation: Onset of Fragmentation of Polyethylene Films in Marine Environment Mesocosms, *Front. Mar. Sci.*, 2017, **4**, 84.

8 L. M. Hernandez, J. Grant, P. S. Fard, J. M. Farner and N. Tufenkji, Analysis of ultraviolet and thermal degradations of four common microplastics and evidence of nanoparticle release, *J. Hazard. Mater. Lett.*, 2023, **4**, 100078.

9 E.-L. Ng, E. H. Lwanga, S. M. Eldridge, P. Johnston, H.-W. Hu, V. Geissen and D. Chen, An overview of microplastic and nanoplastic pollution in agroecosystems, *Sci. Total Environ.*, 2018, **627**, 1377–1388.

10 M. Scheurer and M. Bigalke, Microplastics in Swiss Floodplain Soils, *Environ. Sci. Technol.*, 2018, **52**, 3591–3598.

11 S. Zhang, X. Yang, H. Gertsen, P. Peters, T. Salánki and V. Geissen, A simple method for the extraction and identification of light density microplastics from soil, *Sci. Total Environ.*, 2018, **616**, 1056–1065.

12 B.-K. Zhu, Y.-M. Fang, D. Zhu, P. Christie, X. Ke and Y.-G. Zhu, Exposure to nanoplastics disturbs the gut microbiome in the soil oligochaete *Enchytraeus crypticus*, *Environ. Pollut.*, 2018, **239**, 408–415.

13 C.-Q. Zhou, C.-H. Lu, L. Mai, L.-J. Bao, L.-Y. Liu and E. Y. Zeng, Response of rice (*Oryza sativa* L.) roots to nanoplastic treatment at seedling stage, *J. Hazard. Mater.*, 2021, **401**, 123412.

14 M. Davranche, C. Veclin, A.-C. Pierson-Wickmann, H. El Hadri, B. Grassl, L. Rowenczyk, A. Dia, A. Ter Halle, F. Blancho, S. Reynaud and J. Gigault, Are nanoplastics able to bind significant amount of metals? The lead example, *Environ. Pollut.*, 2019, **249**, 940–948.

15 L. Liu, R. Fokkink and A. A. Koelmans, Sorption of polycyclic aromatic hydrocarbons to polystyrene nanoplastic, *Environ. Toxicol. Chem.*, 2016, **35**, 1650–1655.

16 J. Gigault, H. El Hadri, B. Nguyen, B. Grassl, L. Rowenczyk, N. Tufenkji, S. Feng and M. Wiesner, Nanoplastics are neither microplastics nor engineered nanoparticles, *Nat. Nanotechnol.*, 2021, **16**, 501–507.

17 B. Nguyen, D. Claveau-Mallet, L. M. Hernandez, E. G. Xu, J. M. Farner and N. Tufenkji, Separation and Analysis of Microplastics and Nanoplastics in Complex Environmental Samples, *Acc. Chem. Res.*, 2019, **52**, 858–866.

18 O. S. Alimi, D. Claveau-Mallet, R. S. Kurusu, M. Lapointe, S. Bayen and N. Tufenkji, Weathering pathways and protocols for environmentally relevant microplastics and nanoplastics: what are we missing?, *J. Hazard. Mater.*, 2022, **423**, 126955.

19 L. Rowenczyk, A. Dazzi, A. Deniset-Besseau, V. Beltran, D. Goudounèche, P. Wong-Wah-Chung, O. Boyron, M. George, P. Fabre, C. Roux, A. F. Mingotaud and A. t. Halle, Microstructure Characterization of Oceanic Polyethylene Debris, *Environ. Sci. Technol.*, 2020, **54**, 4102–4109.

20 C. J. Garvey, M. Impérator-Clerc, S. Rouzière, G. Gouadec, O. Boyron, L. Rowenczyk, A. F. Mingotaud and A. ter Halle, Molecular-Scale Understanding of the Embrittlement in Polyethylene Ocean Debris, *Environ. Sci. Technol.*, 2020, **54**, 11173–11181.

21 Y. K. Song, S. H. Hong, M. Jang, G. M. Han, S. W. Jung and W. J. Shim, Combined effects of UV exposure duration and mechanical abrasion on microplastic fragmentation by polymer type, *Environ. Sci. Technol.*, 2017, **51**, 4368–4376.

22 A. Singh and M. Agrawal, Acid rain and its ecological consequences, *J. Environ. Biol.*, 2007, **29**, 15.

23 Y. Zhao, Z. Han, Y. Xie, X. Fan, Y. Nie, P. Wang, G. Liu, Y. Hao, J. Huang and W. Zhu, Correlation Between Thermal Parameters and Morphology of Cross-Linked Polyethylene, *IEEE Access*, 2020, **8**, 19726–19736.

24 PerkinElmer, *Characterization of Polymers Using TGA*, 2011.

25 V. B. F. Mathot, Temperature dependence of some thermodynamic functions for amorphous and semi-crystalline polymers, *Polymer*, 1984, **25**, 579–599.

26 J. V. Gulmine, P. R. Janissek, H. M. Heise and L. Akcelrud, Polyethylene characterization by FTIR, *Polym. Test.*, 2002, **21**, 557–563.

27 A. Ter Halle, L. Ladirat, M. Martignac, A. F. Mingotaud, O. Boyron and E. Perez, To what extent are microplastics from the open ocean weathered?, *Environ. Pollut.*, 2017, **227**, 167–174.

28 E. Cernia, C. Mancini and G. Montaudo, Contribution to the investigation of polyethylene by infrared techniques, *J. Polym. Sci., Part B: Polym. Lett.*, 1963, **1**, 371–377.

29 F. Carrasco, P. Pagès, S. Pascual and X. Colom, Artificial aging of high-density polyethylene by ultraviolet irradiation, *Eur. Polym. J.*, 2001, **37**, 1457–1464.

30 J. V. Gulmine, P. R. Janissek, H. M. Heise and L. Akcelrud, Degradation profile of polyethylene after artificial accelerated weathering, *Polym. Degrad. Stab.*, 2003, **79**, 385–397.

31 D. Oldak, H. Kaczmarek, T. Buffeteau and C. Sourisseau, Photo- and Bio-Degradation Processes in Polyethylene, Cellulose and their Blends Studied by ATR-FTIR and Raman Spectroscopies, *J. Mater. Sci.*, 2005, **40**, 4189–4198.

32 M. Gardette, A. Perthue, J.-L. Gardette, T. Janecska, E. Földes, B. Pukánszky and S. Therias, Photo- and thermal-oxidation of polyethylene: comparison of



mechanisms and influence of unsaturation content, *Polym. Degrad. Stab.*, 2013, **98**, 2383–2390.

33 J. Pilař, M. Šlouf, D. Michálková, I. Šloufová, T. Vacková and J. Dybal, Pro-oxidant activity of  $\alpha$ -tocopherol during photooxidative degradation of polyolefins. ESRI and IR microspectroscopy studies, *Polym. Degrad. Stab.*, 2017, **138**, 55–71.

34 P. Gijsman, J. Hennekens and D. Tummers, The mechanism of action of hindered amine light stabilizers, *Polym. Degrad. Stab.*, 1993, **39**, 225–233.

35 J. Almond, P. Sugumaar, M. N. Wenzel, G. Hill and C. Wallis, Determination of the carbonyl index of polyethylene and polypropylene using specified area under band methodology with ATR-FTIR spectroscopy, *e-Polym.*, 2020, **20**, 369–381.

36 G. Grause, M.-F. Chien and C. Inoue, Changes during the weathering of polyolefins, *Polym. Degrad. Stab.*, 2020, **181**, 109364.

37 S. Wu, Z. Chen, M. Zhou, Y. Shao, C. Jin, J. Tang, F. Fang, J. Guo, F. Stibany and A. Schäffer, Freeze-thaw alternations accelerate plasticizers release and pose a risk for exposed organisms, *Ecotoxicol. Environ. Saf.*, 2022, **241**, 113742.

38 M. Tadros, P. Hu and A. Adamson, Adsorption and contact angle studies: I. Water on smooth carbon, linear polyethylene, and stearic acid-coated copper, *J. Colloid Interface Sci.*, 1974, **49**, 184–195.

39 H. Bockhorn, A. Hornung, U. Hornung and D. Schawaller, Kinetic study on the thermal degradation of polypropylene and polyethylene, *J. Anal. Appl. Pyrolysis*, 1999, **48**, 93–109.

40 J. D. Peterson, S. Vyazovkin and C. A. Wight, Kinetics of the Thermal and Thermo-Oxidative Degradation of Polystyrene, Polyethylene and Poly(propylene), *Macromol. Chem. Phys.*, 2001, **202**, 775–784.

41 C. P. Ward and C. M. Reddy, We need better data about the environmental persistence of plastic goods, *Proc. Natl. Acad. Sci. U. S. A.*, 2020, **117**, 14618–14621.

42 N. M. Stark and L. M. Matuana, Surface chemistry and mechanical property changes of wood-flour/high-density-polyethylene composites after accelerated weathering, *J. Appl. Polym. Sci.*, 2004, **94**, 2263–2273.

43 F. Julianne, N. Delorme and F. Lagarde, From macroplastics to microplastics: role of water in the fragmentation of polyethylene, *Chemosphere*, 2019, **236**, 124409.

44 Y. Lv, Y. Huang, J. Yang, M. Kong, H. Yang, J. Zhao and G. Li, Outdoor and accelerated laboratory weathering of polypropylene: a comparison and correlation study, *Polym. Degrad. Stab.*, 2015, **112**, 145–159.

45 Y. Lv, Y. Huang, M. Kong, Q. Yang and G. Li, Multivariate correlation analysis of outdoor weathering behavior of polypropylene under diverse climate scenarios, *Polym. Test.*, 2017, **64**, 65–76.

46 J.-W. Wee, M.-S. Choi, H.-C. Hyun, J.-H. Hwang and B.-H. Choi, Effect of weathering-induced degradation on the fracture and fatigue characteristics of injection-molded polypropylene/talc composites, *Int. J. Fatig.*, 2018, **117**, 111–120.

47 S. G. Hirsch, B. Barel, D. Shpasser, E. Segal and O. M. Gazit, Correlating chemical and physical changes of photo-oxidized low-density polyethylene to the activation energy of water release, *Polym. Test.*, 2017, **64**, 194–199.

48 M. C. L. Belone, M. Kokko and E. Sarlin, The effects of weathering-induced degradation of polymers in the microplastic study involving reduction of organic matter, *Environ. Pollut.*, 2022, **308**, 119669.

49 S. F. Chabira, M. Sebaa and C. G'Sell, Influence of climatic ageing on the mechanical properties and the microstructure of low-density polyethylene films, *J. Appl. Polym. Sci.*, 2008, **110**, 2516–2524.

50 K. Zhang, A. H. Hamidian, A. Tubić, Y. Zhang, J. K. Fang, C. Wu and P. K. Lam, Understanding plastic degradation and microplastic formation in the environment: a review, *Environ. Pollut.*, 2021, **274**, 116554.

51 S. S. Ali, T. Elsamahy, E. Koutra, M. Kornaros, M. El-Sheekh, E. A. Abdelkarim, D. Zhu and J. Sun, Degradation of conventional plastic wastes in the environment: a review on current status of knowledge and future perspectives of disposal, *Sci. Total Environ.*, 2021, **771**, 144719.

